



Estimating water discharge from large radar altimetry datasets

A. C. V. Getirana and C. Peters-Lidard

Hydrological Sciences Laboratory, NASA Goddard Space Flight Center, Greenbelt, MD 20771, USA

Correspondence to: A. C. V. Getirana (augusto.getirana@nasa.gov)

Received: 28 May 2012 – Published in Hydrol. Earth Syst. Sci. Discuss.: 14 June 2012

Revised: 4 February 2013 – Accepted: 14 February 2013 – Published: 4 March 2013

Abstract. The objective of this study is to evaluate the potential of large altimetry datasets as a complementary gauging network capable of providing water discharge in ungauged regions. A rating curve-based methodology is adopted to derive water discharge from altimetric data provided by the Envisat satellite at 475 virtual stations (VS) within the Amazon basin. From a global-scale perspective, the stage–discharge relations at VS are built based on radar altimetry and outputs from a modeling system composed of a land surface model and a global river routing scheme. In order to quantify the impact of model uncertainties on rating-curve based discharges, a second experiment is performed using outputs from a simulation where daily observed discharges at 135 gauging stations are introduced in the modeling system. Discharge estimates at 90 VS are evaluated against observations during the curve fitting calibration (2002–2005) and evaluation (2006–2008) periods, resulting in mean normalized RMS errors as high as 39 and 15 % for experiments without and with direct insertion of data, respectively. Without direct insertion, uncertainty of discharge estimates can be mostly attributed to forcing errors at smaller scales, generating a positive correlation between performance and drainage area. Mean relative streamflow volume errors (RE) of altimetry-based discharges varied from 15 to 84 % for large and small drainage areas, respectively. Rating curves produced a mean RE of 51 % versus 68 % from model outputs. Inserting discharge data into the modeling system decreases the mean RE from 51 to 18 %, and mean NRMSE from 24 to 9 %. These results demonstrate the feasibility of applying the proposed methodology to the continental or global scales.

1 Introduction

In the last decades, the hydrological sciences community has experienced significant advances in the understanding of water storage and transport over the continents using remote sensing data. In particular, radar altimetry, firstly designed to monitor the oceans, has motivated the development of techniques attempting to improve our understanding of inland water fluxes worldwide. It has been shown that radar altimetry, in the form of virtual stations, or VS (defined as the location where satellite ground tracks transect open-water surfaces), can significantly contribute to the monitoring of poorly gauged or ungauged areas. Most applications have attempted to retrieve water discharges from stage–discharge relations derived from altimetric data and observed discharges from gauging stations located in the vicinity of the VS. These relations are commonly represented by rating curves and allow one to predict water discharges from observed water levels, with accuracy varying as a function of input data and flow regime characteristics. As examples, river discharges have been estimated from altimetric data in the Chari River (Coe and Birkett, 2004), Ob’ River (Kouraev et al., 2004), Amazon River (Zakharova et al., 2006) and Zambezi River (Michailovsky et al., 2012). Although errors between predicted and observed water discharges are relatively small in most applications, the use of such methods is restricted to VS located near gauging stations. Other studies have taken advantage of radar altimetry data to make forecasts at gauges downstream of a virtual station. Coe and Birkett (2004) first suggested and applied this idea to forecast downstream discharges and levels in Lake Chad. Then, similar approaches have been applied in a few other studies to forecast downstream discharges in the Mekong River (Birkinshaw et al., 2010) and downstream water levels in the Ganges and Brahmaputra Rivers (Biancamaria et al., 2011).

Some studies preparing for the upcoming Surface Water Ocean Topography Mission (SWOT; Alsdorf et al., 2007) have combined virtual swath altimetric measurements with hydrodynamic models in a data assimilation framework in order to improve river depth and discharge (e.g. Andreadis et al., 2007; Durand et al., 2008). These studies show the potential of upcoming altimetric measurements and the expected improvements in estimating discharges, river geometry and roughness parameters in ungauged basins.

Recent works in the Amazon basin have addressed current limitations such as the need for observed discharges and river cross sectional information at VS by using rating curves and discharge estimates derived from routing schemes (León et al., 2006) and rainfall-runoff models (Getirana et al., 2009) at the regional scale. These hydrologic models are generally calibrated for a specific river reach or region, providing accurate discharge simulations and reducing the uncertainty introduced in approaches combining both radar altimetry data and discharges. León et al. (2006) attempted to determine riverbed heights and Manning roughness coefficients from curve fitting parameters while Getirana et al. (2009) evaluated the potential of estimating discharges from radar altimetry data using rating curves. Another study performed by Getirana (2011) introduced a rating curve model into an optimization scheme in order to drive the automatic calibration of a rainfall-runoff model exclusively using radar altimetry data.

A recent effort in acquiring altimetric data resulted in an unprecedented radar altimetry dataset at several hundreds of virtual stations over the main lakes, rivers and tributaries on the planet (<http://www.legos.obs-mip.fr/soa/hydrologie/hydroweb/>), hereafter called the Hydroweb dataset (Crétaux et al., 2011). In addition, recent studies have focused on the development of more precise global modeling systems capable of simulating continental water fluxes (e.g. Doll et al., 2003; Kumar et al., 2006; Decharme et al., 2010). On the other hand, even though the Amazon basin is responsible for about 15 % of the water flow from continents to oceans, it is poorly gauged and its hydrological processes are still unknown in many areas at the meso and regional scales. Taking advantage of the Hydroweb dataset and recent advances in global scale hydrological modeling, the present study extends the application of the rating curve approach at the continental scale, investigating whether it is possible to estimate instantaneous discharges from current large scale radar altimetry datasets and quantifying their accuracy. Specifically, this study evaluates a methodology where stage–discharge relations are based on rating curves derived from Envisat data and simulated discharges provided by the Hydrological Modeling and Analysis Platform (HyMAP) flow routing scheme (Getirana et al., 2012) coupled in off-line mode with the Interactions Sol-Biosphère-Atmosphère (ISBA) (Noilhan and Mahfouf, 1996) land surface model (LSM). The results of this study point toward a general methodology capable of predicting water discharges at the continental or global

scale from the next generation of satellite missions such as the SWOT mission.

2 The stage–discharge relation

The stage–discharge relation is a hydraulic property of a river reach or cross section and it is unknown a priori. The hydrologist must define it based on an approximated representation by a rating curve, traditionally built based on in situ measurements and supported by the analysis of streamflow parameters (Jacon and Cudo, 1989). In general, the rating curve of a specific river location can be expressed by mathematical expressions representing successive linear reaches or curves. The most frequently used form is the exponential one defined as $Q = a \cdot h^b$, where Q [$\text{m}^3 \text{s}^{-1}$] is the estimated discharge and h [m] the water depth related to a given zero-flow-equivalent water height, z (see below for details). In general, the coefficient a reproduces the relief of the river reaches, including surface roughness and sinuosity, and b the geometry of riverbanks (Rantz et al., 1982). If the Manning equation for wide rectangular channels is considered as a reasonable representation of the truth, these coefficients can be expressed as $a = w \cdot S_o^{1/2} \cdot n^{-1}$ and $b = 5/3$, where w is the river width, S_o the river slope and n the river flow roughness coefficient. However, as in most applications, a and b are estimated by curve-fitting, and they do not necessarily represent their physical characteristics. Due to changes in the river geometry, rating curves must be updated periodically. Also, scatter around the curve can exist as the relation is derived from approximations of observations. Errors can be on the order of 10–15 %, varying as a function of the river geometry, numerical approximation and quantity and quality of measurements. Feasible S_o values found at virtual stations within the study area can range from 10^{-6} to $0.1 \text{ m} \cdot \text{m}^{-1}$ (in practice, river reaches located in flat areas can have zero slopes and the lower bound was defined in order to constrain the estimation of a , as described below), and w [m] can vary from 100 to 10 km. Chow (1959) lists Manning roughness coefficients for open channels, suggesting that feasible n values can vary from 0.01 to 0.16. In this sense, one can say that feasible a values can range from 1 to 10^5 .

Radar altimetry provides us with the height, H [m], which represents the instantaneous measurement of the Earth's surface height referenced to a specified ellipsoid. In this sense, H corresponds to the height of the reflecting surface that receives and reflects the satellite radar echoes. The river depth h can be derived from H by subtracting the mean river bed elevation, or the zero-flow water height, z ($h = H - z$). This leads to the general formulation of the rating curve equation defined as

$$Q = a \cdot (H - z)^b. \quad (1)$$

However, as in most cases, the zero-flow water height z is an unknown variable. A straightforward way to estimate this

parameter is by minimizing errors of curve-fitting between stage and discharge observations at a given location and period using the linear form of Eq. (1):

$$\ln(Q) = \ln(a) + b \cdot \ln(H - z). \quad (2)$$

3 Methods

The methodology used to predict water discharges is based on rating curve fitting by combining radar altimetry with simulated discharges in Eq. (2) and is similar to those applied in León et al. (2006) and Getirana et al. (2009). Coefficients a , b and z are calibrated for each VS in two steps. First, a set of a and b coefficients are defined based on the best fit between Q and $H-z$, where z ranges from the minimum altimetric observation (H_{\min}) to 50 m b.s.l. (below sea level) (this value was used in order to assure the existence of any feasible z value). The range of possible z values has been explored by increments of 0.01 m. The curve fitting for each z value is based on the minimization of the sum of squared residuals of the linear regression model of Eq. (2).

The best z value is then obtained by maximizing the coefficient of determination, R^2 . R^2 is computed for the best fit between Q and $H - z$, as denoted by Eq. (2), and ranges between zero and 1, where 1 represents the optimal value. Exploring the range of possible values of z allows the function $R^2 = f(z)$ to be built up. The optimization of R^2 is constrained by the feasible values defined for a , ranging from 1 to 10^5 (see Sect. 2). In cases where convergence is not reached, i.e. $R^2 = f(z = \infty)$, the search procedure stops when a differential $R^2(dR^2)$ between two search steps is equal or less than 10^{-6} . These cases will be called “non-converging curve fittings” hereafter (and the opposite case “converging curve fittings”).

3.1 Envisat altimetry data

Envisat orbits on a 35-day temporal resolution (duration of the orbital cycle) from latitude 81.5° N to 81.5° S, and 70 km inter-track spacing at the Equator. Its beam footprint width is about 3.5 km. The radar altimetry dataset used in this study is the one available on Hydroweb (Crétau et al., 2011). The Envisat radar altimetry dataset covers several large rivers, lakes and floodplains within the Amazon basin, being composed of over 1500 VS. After selection of VS located over rivers with sufficiently long and consistent time series, 475 VS remained (see Fig. 1 for the spatial distribution of VS). The ranges used in this study are those issued by the ICE-1 algorithm (Bamber, 1994). Absolute errors of altimetric time series within the Amazon basin are in the order of tens of centimeters (Silva et al., 2011). Selected VS cover most Amazon River’s tributaries and other small rivers, with drainage areas ranging from 10 000 to 5 238 800 km². Time series length varies from 23 to 63 altimetric observations

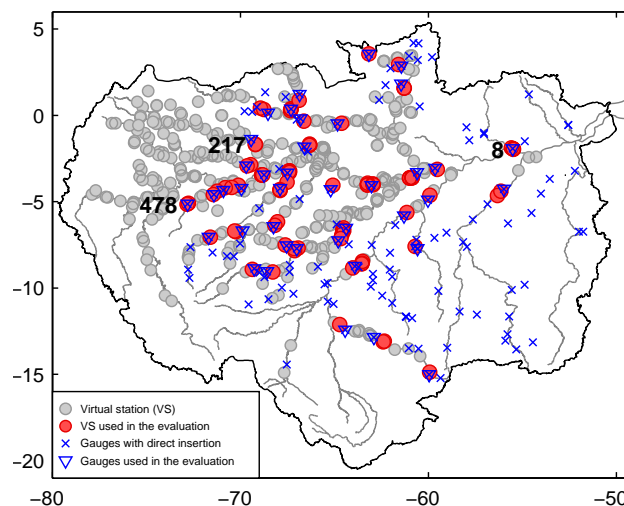


Fig. 1. The Amazon basin and the geographical location of virtual and gauging stations used in this study.

for the 2002–2009 period. Details about the data extraction technique, retracking and evaluation against in situ observations are reported in Silva et al. (2011). In this study, the water heights provided by Envisat were converted to altitudes using the GRACE static solution of GGM02C geoid model (Tapley et al., 2004).

3.2 The HyMAP river routing scheme

Simulated discharges (Q_{sim}) are provided at a daily time step and 0.25° spatial resolution by HyMAP, coupled in off-line mode with ISBA (Noilhan and Mahfouf, 1996). HyMAP is a global scale flow routing scheme capable of simulating flow velocity, water discharge, depth and storage in rivers and floodplains, among other hydrological variables. The runoff and baseflow generated by ISBA (see Decharme et al., 2012 for a full description of ISBA parameterization and forcings) are routed using a kinematic wave formulation through a prescribed river network to oceans or inland seas. The model is fully described and evaluated in Getirana et al. (2012).

HyMAP simulates water level, discharge and storage in rivers and floodplains at the spatial resolution of 0.25° and at the daily time step. For this study, the internal computational time step was set as 15 min. The surface and subsurface runoff s generated by a LSM are routed using a kinematic wave formulation through a prescribed river network to oceans or inland seas. The model is composed of four modules accounting for (1) the surface and subsurface runoff time delays, (2) flow routing in river channels, (3) flow routing in floodplains and (4) evaporation from open water surfaces. Although the kinematic wave equation may not be adequate for river reaches under unsteady flow conditions (Trigg et al., 2009), recent modeling attempts in the Amazon basin using different approaches and datasets suggest that

(1) meteorological forcings (mainly precipitation), (2) the simulated vertical water balance and (3) observed data used in the evaluation process have a higher impact on simulated discharges than the routing method itself. In addition, according to a comparison performed by Yamazaki et al. (2011) at the global scale, only small differences in discharges simulated by both kinematic and diffusive wave formulations were found. According to Getirana et al. (2012), 23 % of the stream gauges considered in the evaluation have Nash–Sutcliffe (NS) coefficients higher than 0.50 and 68 % above zero. Also, discharges are very well simulated at Óbidos, with $NS = 0.89$.

The uncertainty of simulated discharge varies spatially as a function of both the size the drainage area (A) and quality of LSM inputs, notably the precipitation field. The relative streamflow volume error (RE) of simulated discharges ranges from 0.155 (or 15.5 %) for large basins ($A > 10^6 \text{ km}^2$) to 1.105 ($\sim 110\%$) for smaller areas ($A < 10^5 \text{ km}^2$). RE values are closely related to the vertical water balance, which is highly sensitive to precipitation and LSM parameterization.

Two experiments were performed in order to evaluate the impacts of simulated discharge uncertainties on rating curve fitting. The first one uses simulated discharge from the default HyMAP model configuration as described in Getirana et al. (2012). The second one takes advantage of observed daily discharges (Q_{obs}) at 135 gauging stations (see spatial distribution of stations in Fig. 1) during the HyMAP run by directly replacing simulated discharges with observations at the outlet of the corresponding grid cells. Experiments 1 and 2 will be also called “default simulation” and “direct insertion”. Gauging stations are operated by the Brazilian Water Agency (ANA) and have at least one year of observed discharges within the study period. The discharge data replacement assures that uncertainties in the curve fitting at VS located near gauging stations are mainly due to altimetric data rather than discharge. Finally, two different discharge estimate time series can be provided by rating curves at each VS: (1) discharge derived from curve fitting without data replacement (Q_{rc0}); and (2) with data replacement (Q_{rc1}). Curve fitting was performed during the 2002–2005 calibration period for the whole set of VS. However, only 90 VS located near gauging stations had discharge estimates compared against observations. In order to quantify the impacts of radar altimetry data on discharge estimates from rating curves, H_{sat} at these same selected virtual stations was compared to stage observations for both calibration and evaluation periods. The distances between the selected VS and gauging stations do not exceed 30 km. Based on the geographical proximity, it was considered that these stations have the same hydrological response, since the incremental area within the reaches are irrelevant if compared to the total drainage areas upstream the stations.

The evaluation of predicted water discharges by rating curves was performed in the 2006–2008 period. The accuracy of discharge estimates was determined by using three

performance coefficients: the normalized root mean square error (NRMSE), the Nash–Sutcliffe (NS) coefficient and the relative streamflow volume error (RE).

$$\text{NRMSE} = \frac{\text{RMSE}}{(y_{\text{max}} - y_{\text{min}})} \quad (3)$$

$$\text{NS} = 1 - \frac{\sum_{t=1}^{nt} (y_t - x_t)^2}{\sum_{t=1}^{nt} (y_t - \bar{y})^2} \quad (4)$$

$$\text{RE} = \frac{\sum_{t=1}^{nt} x_t - \sum_{t=1}^{nt} y_t}{\sum_{t=1}^{nt} y_t} \quad (5)$$

where t is the time step, nt the total number of days disposing of observed data, x and y are, respectively, the simulated and target (observed) signals at time step t , and y_{max} , y_{min} and \bar{y} , are respectively, the maximum, minimum and mean values of the target signals for the entire period. NS ranges from $-\infty$ to 1, where 1 is the optimal case and zero is when simulations represent observed signals as well as the mean value. NRMSE and RE vary from -1 to $+\infty$, where zero is the optimal case. One can obtain NRMSE and RE values in percentage by multiplying them by 100.

4 Results and discussion

4.1 Curve fitting

Figure 2 shows the spatial distribution of R^2 values and curve coefficients (a , b and z) derived from the calibration procedure for both experiments. For experiment 1 (default simulation), from a total of 475 VS, 225 had rating curves converging to optimal z values. The other 250 VS had the calibration procedure interrupted based on the $dR^2 \leq 10^{-6}$ criterion or constrained by feasible a values, as discussed above. R^2 values used as the objective function in the calibration varied from zero to 0.95. 87 VS had $R^2 \leq 0.20$. These VS are mostly located in the Western Amazon basin and represent small catchments. The mean R^2 value of converging rating curves was 0.49. Diverging rating curves had a higher mean R^2 of 0.67, which implies that non-convergence does not necessarily indicate bad curve fitting. This deduction will be addressed in the next section. The mean R^2 for the entire set of VS was 0.57.

As for experiment 2 (direct insertion), 324 rating curves converged to optimal z values, representing an increase of 44 % in comparison with experiment 1. The inclusion of water discharge observations in the modeling system also improved R^2 values, varying from zero to ~ 1 . Converging and diverging curve fittings had mean R^2 of 0.71 and 0.66, respectively. The mean R^2 for the 475 VS was 0.69. Improvements are clearly noticed downstream of gauging

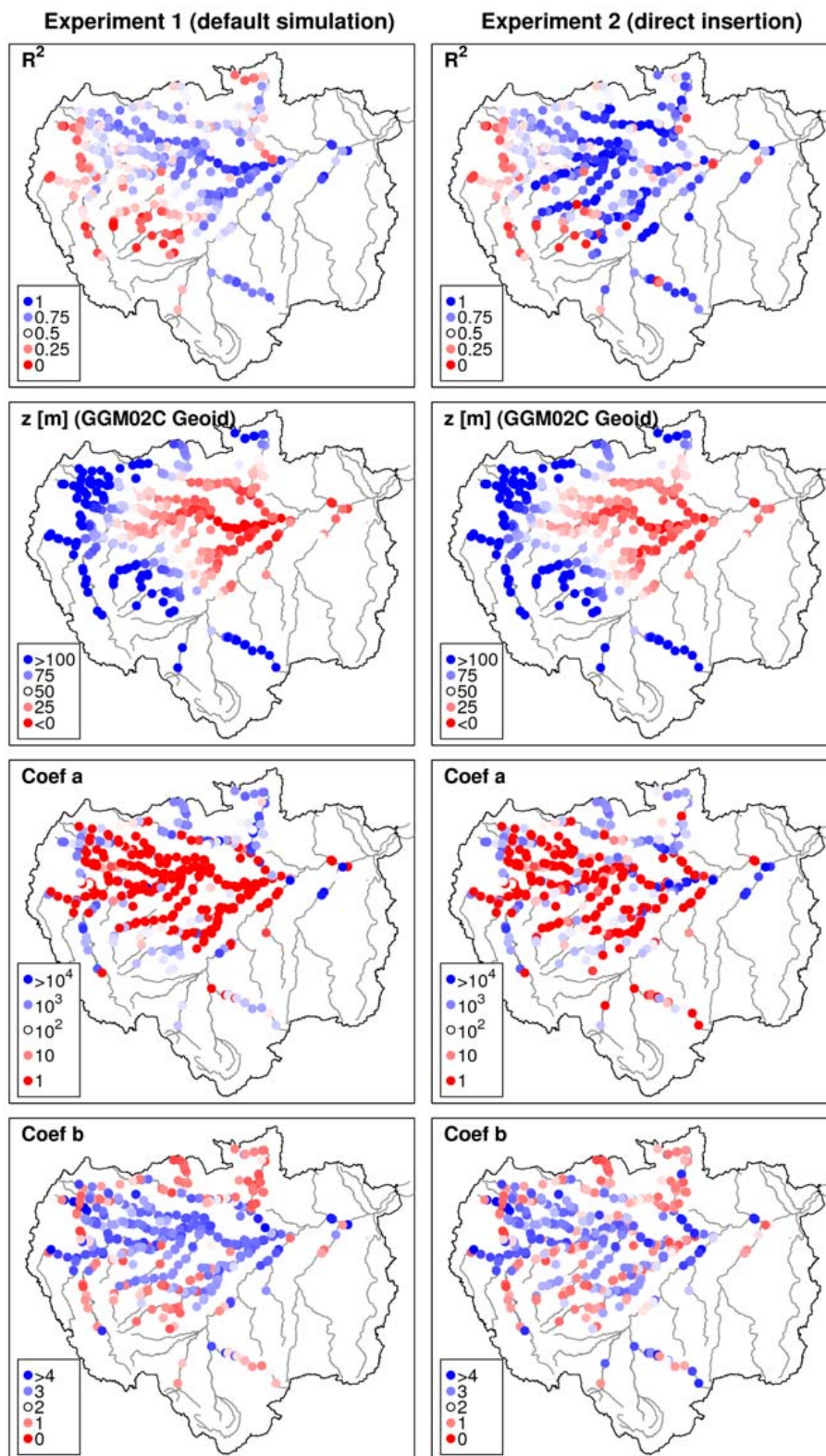


Fig. 2. Results of curve fitting at 475 virtual stations. Zero-flow equivalent depth (z) values and coefficients a and b are omitted (represented by crossed circles) at virtual stations with non-converging rating curves.

Table 1. Performance coefficients (NRMSE, RE and NS) of water discharges estimated by the rating curves at selected virtual stations for the calibration period (2002–2005). Coefficients of modeled discharges at gauging stations used in the evaluation are also provided. Values correspond to averages of drainage area thresholds.

| | Thresholds of drainage area, A (km ²) | | | |
|--------------------------------|---|-------------------|------------|-------|
| | $A < 10^5$ | $10^5 < A < 10^6$ | $A > 10^6$ | Total |
| Experiment 1 (Q_{rc0}) | | | | |
| NRMSE | 0.37 | 0.20 | 0.13 | 0.24 |
| RE | 0.84 | 0.49 | 0.15 | 0.51 |
| NS | -1.81 | 0.26 | 0.77 | -0.23 |
| Experiment 2 (Q_{rc1}) | | | | |
| NRMSE | 0.07 | 0.09 | 0.11 | 0.09 |
| RE | 0.15 | 0.24 | 0.11 | 0.18 |
| NS | 0.92 | 0.83 | 0.80 | 0.85 |
| HyMAP simulation (Q_{sim}) | | | | |
| NRMSE | 0.37 | 0.25 | 0.13 | 0.26 |
| RE | 1.11 | 0.63 | 0.16 | 0.68 |
| NS | -1.32 | 0.17 | 0.77 | -0.16 |

stations, especially in small and medium rivers. These results demonstrate a significant enhancement in the curve calibration when observed discharges are inserted in the modeling system.

According to Fig. 2, the zero-flow equivalent depth, z , and coefficients a and b had similar values for both experiments. Overall, z values are physically consistent at VS where the calibration converged, ranging from -1.45 and from -5.54 m (experiments 1 and 2, respectively) near Óbidos to about 314 and 313 m in the western Amazon basin, near the Andes Mountains. Both coefficients a and b showed large ranges. The coefficient a ranged from 1 to about 21 800, while b varied from 0.35 to 6.41. As these values result from an automatic calibration procedure, their physical meanings remain unclear and are not discussed in this study.

4.2 Accuracy of discharge estimates

Tables 1 and 2 list the performance coefficients (NRMSE, RE and NS) used to evaluate the accuracy of discharge estimates provided by the rating curves and modeling during the calibration and evaluation periods. Coefficients are presented as averages of drainage area (A) thresholds: small ($A < 10^5$ km²); medium (10^5 km² < $A < 10^6$ km²); and large ($A > 10^6$ km²) drainage areas.

Although discharge estimates derived from experiment 1 (Q_{rc0}) had overall poor results (NRMSE = 24 %, RE = 51 % and NS = -0.23), performance coefficients can vary as a function of the drainage area. Virtual stations with smaller areas had discharge estimates with low accuracy (37 %,

Table 2. Same as Table 1, but for the validation period (2006–2008). Simulated discharges are not available for this entire period.

| | Thresholds of drainage area, A (km ²) | | | |
|----------------------------|---|-------------------|------------|-------|
| | $A < 10^5$ | $10^5 < A < 10^6$ | $A > 10^6$ | Total |
| Experiment 1 (Q_{rc0}) | | | | |
| NRMSE | 0.38 | 0.22 | 0.15 | 0.25 |
| RE | 0.84 | 0.44 | 0.15 | 0.48 |
| NS | -1.22 | 0.26 | 0.67 | -0.06 |
| Experiment 2 (Q_{rc1}) | | | | |
| NRMSE | 0.09 | 0.10 | 0.14 | 0.11 |
| RE | 0.15 | 0.20 | 0.12 | 0.17 |
| NS | 0.85 | 0.84 | 0.67 | 0.80 |

84 % and -1.81, respectively), while those draining medium (20 %, 49 % and 0.26) and large areas (13 %, 15 % and 0.77) provided much better results. Figure 3 shows NRMSE of selected VS as a function of the drainage area (A). Results of both experiments 1 and 2 are presented for the calibration period. According to the map in the right side of the figure, a larger concentration of VS with high errors is located in the Western side of the basin. These results agree with the spatial distribution of performance coefficients for simulated discharge (Q_{sim}), revealing a positive correlation of 0.26 between the accuracy of Q_{rc0} and Q_{sim} .

A substantial improvement is obtained with the inclusion of discharge data into the modeling system performed in experiment 2. The mean values of coefficients NRMSE and RE for the set of 90 VS were reduced to 9 and 18 %, respectively, and NS had a non-negligible increase to 0.85. Mean NRMSE values for small, medium and large areas are 7, 9 and 11 %, respectively.

Q_{rc1} uncertainty can be mostly attributed to radar altimetry errors since curve fitting was performed using observed discharge. Although the NRMSE values of unbiased Envisat water levels can exceed 20 % for a single VS, the mean NRMSE is 7.4 % for all VS within the Amazon basin, varying from about 7 % for VS draining medium and large areas to 9 % for small areas (Fig. 3). Another source of errors can be curve approximations. The methodology applied in this study is based on the calibration of coefficients (a , b and z) of a single rating curve by maximizing R^2 . Rating curves used by ANA may have been built using different criteria also considering river slope, which represent loop ratings caused by unsteady flow regimes.

Discharge estimated in the evaluation period performed almost as well as estimates in the calibration period, exhibiting only a minor degradation of most coefficients (see Table 2). In experiment 1, mean NRMSE and RE remained nearly the same (25 and 48 %, respectively) with some variation within VS groups. The mean Nash–Sutcliffe coefficient presented a slight improvement (NS = -0.06), explained by

Table 3. Rating curve equations and coefficients of determination R^2 for virtual stations VS-8, VS-217 and VS-478 shown in Fig. 4.

| | Experiment 1 | Experiment 2 |
|--------|--|---|
| vs-8 | $Q_{rc0} = 1.0 \cdot (H + 7.5)^{3.81}$ $R^2 = 0.92$ | $Q_{rc1} = 1.0 \cdot (H + 6.3)^{3.75}$ $R^2 = 0.99$ |
| vs-217 | $Q_{rc0} = 1.0 \cdot (H - 25.2)^{3.25}$ $R^2 = 0.85$ | $Q_{rc1} = 99.4 \cdot (H - 34.6)^{2.22}$ $R^2 = 0.93$ |
| vs-478 | $Q_{rc0} = 428.5 \cdot (H - 67.2)^{0.55}$ $R^2 = 0.47$ | $Q_{rc1} = 30.8 \cdot (H - 66.4)^{1.48}$ $R^2 = 0.99$ |

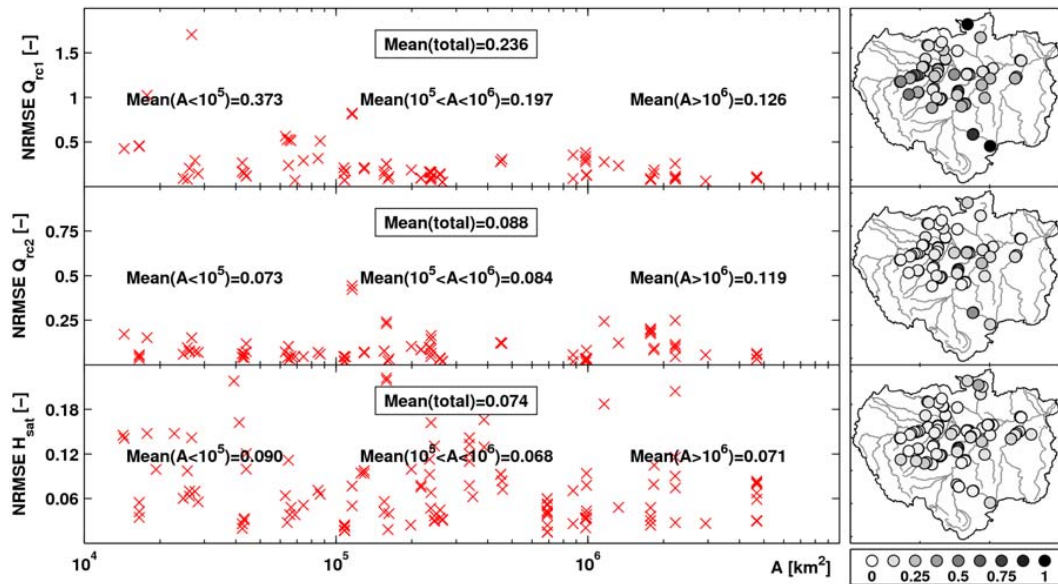


Fig. 3. Normalized root mean square errors (NRMSE) of water discharge and level at 90 virtual stations during the calibration period (2002–2005): on the top, discharge estimates from experiment 1 (no inclusion of observed discharge in the modeling system); in the middle, discharge estimates from experiment 2 (inclusion of observed discharge in the modeling system); and on the bottom, water level fluctuation provided by Envisat. On the left, NRMSE values are presented as functions of the drainage area, A . On the right, NRMSE of virtual stations are spatially distributed within the Amazon basin.

the increasing of the performance at VS with $A < 10^5 \text{ km}^2$. Other groups had NS values lower than those provided by the calibration period. Experiment 2 provided a slight degradation of mean NRMSE, RE and NS (11 %, 17 % and 0.80, respectively) when compared to the calibration period. NRMSE of H_{sat} is slightly higher in the evaluation period (2006–2008), averaging 9 % (not shown). This can explain the general increase of discharge estimate uncertainty in that same period and demonstrates a general agreement with results derived from the calibration period.

Figure 4 shows results of three VS selected from the dataset, each one representing a group of VS defined by drainage areas (see Fig. 1 for location of virtual stations): vs-8 represents a large area, located in the lower Amazon River near Óbidos, drains a surface of $4.7 \times 10^5 \text{ km}^2$ with a mean discharge of $\sim 173\,000 \text{ m}^3 \text{ s}^{-1}$; vs-217 is an example medium area ($209\,200 \text{ km}^2$), located near the Vila Bittencourt station in the Japurá River, mean discharge of $13\,700 \text{ m}^3 \text{ s}^{-1}$; and vs-479 is for small areas ($16\,000 \text{ km}^2$), located near Palmeiras do Javari station in the Javari River, with mean discharge of $620 \text{ m}^3 \text{ s}^{-1}$. At virtual station vs-8,

both curve-fitting experiments did not converge to a feasible z and were stopped based on the dR^2 criterion described in Sect. 3, resulting in maximum R^2 values of 0.92 and 0.99 (see Table 3 for rating curve equations and R^2 values of vs-8, vs-217 and vs-478). The virtual station vs-217 converged in the second curve-fitting experiment only ($z = 34.6 \text{ m}$), but R^2 of both experiments were relatively high (0.85 and 0.93, respectively). Finally, vs-478 had converging z values in both experiments with similar values (67.2 and 66.4 m, respectively), but R^2 values significantly different (0.47 and 0.99, respectively). Although the accuracy of curve-based discharge estimates in experiment 1 varied as a function of the drainage area, all the A threshold cases provided improved discharges when compared to Q_{sim} in the calibration period (2002–2005). Q_{rc0} had RE values of 7 % (vs-8), 18 % (vs-217) and 153 % (vs-478) and NRMSE of 9, 9 and 46 %, respectively (see Tables 4 and 5 for performance coefficients in the calibration and evaluation periods of these three stations). The evaluation period (2006–2008) had similar results, with RE values of 8, 12 and 214 % and NRMSE of 10, 8 and 48 %. The direct insertion of observed data improved

Table 4. Performance coefficients NS, RE and NRMSE for the calibration period (2002–2005) for the virtual stations shown in Fig. 4. Q_{rc0} , Q_{rc1} , and Q_{sim} represent the discharge derived from Experiments 1 and 2, and from the default simulation.

| | vs-8 | | | vs-217 | | | vs-478 | | |
|-----------|------|------|-------|--------|------|-------|--------|------|-------|
| | NS | RE | NRMSE | NS | RE | NRMSE | NS | RE | NRMSE |
| Q_{rc0} | 0.91 | 0.07 | 0.09 | 0.89 | 0.18 | 0.09 | -1.03 | 1.53 | 0.46 |
| Q_{rc1} | 0.99 | 0.03 | 0.03 | 0.90 | 0.12 | 0.08 | 0.99 | 0.08 | 0.04 |
| Q_{sim} | 0.82 | 0.10 | 0.11 | 0.65 | 0.28 | 0.14 | -1.77 | 2.28 | 0.49 |

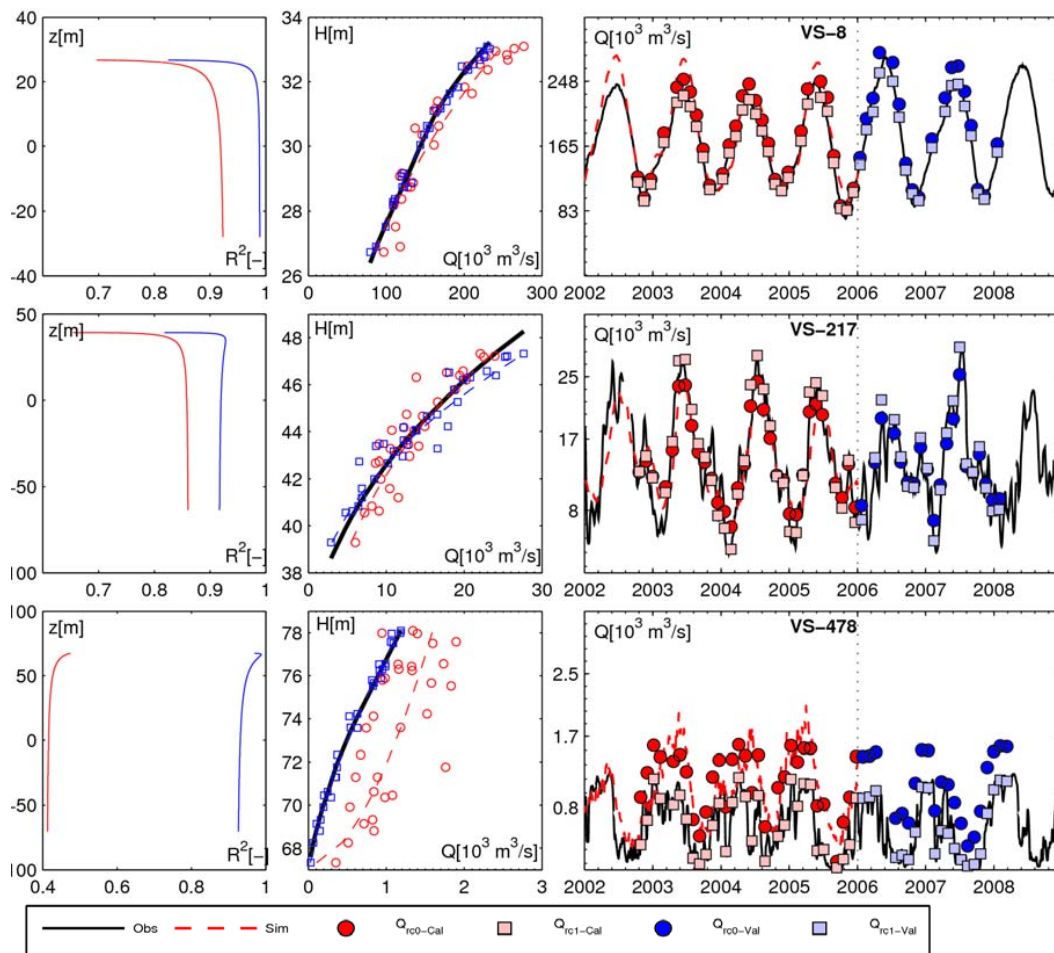


Fig. 4. Results from the curve fitting procedure for three virtual stations: vs-8, vs-217 and vs-478 (see location in Fig. 1). On the left, the optimization of $R^2 = f(z)$: red represents experiment 1 (Q_{rc0}) and blue is experiment 2 (Q_{rc1}). In the middle, the curve fitting for both experiments: red dots and lines stand for experiment 1 and blue squares and lines are derived from experiment 2. On the right, observed and simulated daily discharges and curve estimates for both experiments during the calibration and evaluation periods (legend is provided).

results of all the three VS, but significant changes are evident for vs-478, where RE and NRMSE were drastically improved to 8 and 4 %, respectively, for the calibration period, and 10 and 4 % for the evaluation period. Errors in Q_{rc0} for vs-8 are mainly due to overestimated peak discharge, as provided by HyMAP (see Fig. 4). As for vs-217, Q_{rc0} errors are derived from underestimated peaks, while vs-478 has overestimated discharges throughout the study period.

4.3 Discussion

As mentioned before, discharge estimates derived from rating curves in Experiment 1 (ungauged case) performed overall better than model outputs at stations with medium and large drainage areas. This means that the methodology can be applied in ungauged basins where the evaluation of simulated discharges is not possible. Previous studies, however,

Table 5. The same as Table 4, but for the evaluation period (2006–2008). Simulated discharges (Q_{sim}) are not available for this period.

| | vs-8 | | | vs-217 | | | vs-478 | | |
|------------------|------|------|-------|--------|------|-------|--------|------|-------|
| | NS | RE | NRMSE | NS | RE | NRMSE | NS | RE | NRMSE |
| $Q_{\text{rc}0}$ | 0.91 | 0.08 | 0.10 | 0.88 | 0.13 | 0.08 | −0.70 | 2.14 | 0.48 |
| $Q_{\text{rc}1}$ | 0.98 | 0.03 | 0.04 | 0.89 | 0.09 | 0.08 | 0.99 | 0.10 | 0.04 |

have presented better results in terms of both curve fitting and discharge estimates as discussed below.

León et al. (2006) created rating curves at 21 VS using Envisat and Topex/Poseidon data along the Negro and Uaupes Rivers, located in the Northern Amazon basin. Curve fitting R^2 values varied from 0.66 to 0.99, averaging 0.93. Getirana et al. (2009) presented rating curves at 12 VS in the upper Branco River basin (also located in the Northern Amazon basin) using Envisat data. R^2 values ranged from 0.66 to 0.97, averaging 0.87. According to the results presented in Sect. 4.1, curves are better fitted in the aforementioned studies than in the present one (experiment 1 had minimum, maximum and average R^2 values of zero, 0.95 and 0.57, respectively).

The previous study performed by Getirana's et al. (2009) also evaluated altimetry-based discharges at 3 VS using simulated and observed discharges to retrieve rating curves (similar to experiments 1 and 2 described in this study). The experiment using simulated discharges revealed RE values ranging from 9 to 20 % and RMSE from 11 to 27 %, averaging 13 and 17 %, respectively. In experiment 1 of this study, the same coefficients averaged 24 and 51 %, respectively. The poorer results obtained in the present work can be explained by the (i) modeling approach and (ii) spatial scale. Getirana et al. (2009) used a fully calibrated hydrological model that resulted in NS values between 0.48 and 0.93 (average of 0.72 for eight gauging stations located within the study area), while simulated discharges used in this study had averaged NS values of 0.41 at 119 gauging stations with $\text{NS} \geq 0$ within the Amazon basin. As one of the objectives of this study is to estimate and evaluate the accuracy of water discharge derived from large scale radar altimetry datasets based on rating curves and global modeling systems, both models used to calculate discharges (ISBA and HyMAP) were run with default parameters. As for the spatial scale (ii), Getirana et al. (2009) simulated a small area in the Amazon basin ($\sim 121\,000\text{km}^2$) and evaluated only three altimetry-based discharge time series. This study goes further, evaluating discharge estimates at 90 VS located within the entire basin. On the other hand, one can see that RE and NRMSE values of discharge estimates derived from both experiment 2 and its equivalent experiment performed by Getirana et al. (2009) are comparable (18 and 9 % for the present work and 13 and 17 % for the previous one). Another point that should be discussed is related to the coefficient used in the objective function for the curve fitting. Many measurements can be

considered to evaluate the linear regression of Eq. (2) and curve parameters may change accordingly. As the focus of this study is the evaluation of discharge estimates rather than the reliability of curve parameters, only the coefficient of determination, R^2 , was considered. Therefore, for future works, the use of different measurements is recommended for a full evaluation of curve parameter estimation.

5 Concluding remarks

This study evaluates a methodology to predict water discharges from radar altimetry data with potential applications at the global scale. The technique is based on the calibration of rating curves using altimetric data and simulated water discharge at VS. As a first attempt, the technique was applied to the Amazon basin. Curve fitting coefficients and altimetry-based estimates from 2002 to 2009 were derived at 475 VS within the basin and these entire datasets are available upon request. A first evaluation (called experiment 1) was conducted by building rating curves combining Envisat data and simulated discharges derived from the HyMAP model. In order to evaluate the impacts of model uncertainties on rating curve accuracy, an additional experiment (experiment 2) was performed using model outputs resulting from a discharge data replacement procedure. Discharge estimates at 90 VS were compared against observations at nearby gauging stations. Based on the results obtained, we can say that instantaneous discharge estimates from current large-scale radar altimetry datasets based on rating curves are feasible, but accuracy is highly sensitive to the quality of input data.

Overall, discharge estimates provided by both experiments had good performance. In medium and large rivers, rating curve-based discharges performed better than model simulations. The results are encouraging compared to previous related studies and have errors that are acceptable for most hydrological applications. However, significant differences in experimental results were noted at smaller scales, i.e. VS with drainage areas $A < 10^5\text{ km}^2$, where rainfall monitoring is usually inadequate and model parameter uncertainties are higher (Getirana et al., 2012). Uncertainties of experiment 1 are closely related to simulated discharge errors. This is due to the noise reduction performed by the linear regression. As one could see in Table 1, discharge estimates derived from rating curves in experiment 1 performed overall better than model outputs at stations with medium and large drainage

areas. However, it is clear that the replacement of simulated discharges by observations will improve the overall results. Experiment 2 provided better overall results. The inclusion of observed discharges into the modeling system eliminated the impact of simulated discharges on rating curve accuracy, resulting in a dominant influence of the low altimetric data uncertainty. Such differences between experiments are expected since precipitation and model uncertainties are eradicated by the inclusion of observed data. In some cases where input data are insufficiently accurate to provide a good curve fitting, such as experiment 1 at VS-478 (Fig. 4), the curve parameters may not be reflective of the actual channel hydraulics. This relation will depend on the quality of data used as input for the curve calibration and hydraulic properties of the river at the station. Other cases where parameters may not represent reality occur at locations upstream from a confluence in flat regions. Stations located in these areas may be influenced by backwater effects, which are not considered in the rating curve method.

Even if discharge estimates can be obtained by applying the stage–discharge approach, it is worth noting that the approach ignores the effects of river slope variation and does not guarantee accurate estimation of the discharge in river reaches dominated by unsteady flow regimes. Previous works have shown that steady state assumptions can result in large errors in discharge estimates (Fenton, 2001; Di Baldassarre and Montanari, 2009; Dorotti et al., 2009), but these authors also note that in many cases correction with river slope information may not be necessary.

In this study, river slopes could not be considered in the discharge estimates because this information is not provided by any past or current radar altimeter (except for the occasional cases where the satellite track longitudinally crosses a river reach). Altimetric data at two nearby VS are not measured at the same moment and time lags can be of several days, resulting in inaccurate river slope estimates. As a consequence, river slopes derived from these data can be inappropriate for our purposes. Also, stream gauge data are too sparse to be considered in a generalized methodology. Efforts using minimum values of altimetric observations (H_{\min}) at VS (e.g. Getirana et al., 2009) or combining radar altimetry and gauged data (e.g. Kosuth et al., 2006) have demonstrated the feasibility in estimating river slopes. Further efforts must be made towards the evaluation and application of such methods within an automated framework and at large scales. The forthcoming SWOT mission will provide wide swath water level measurements with the potential for high-resolution characterization of water surface elevations, including river slope. Such promising data availability will allow us to estimate discharges based on slope-based approaches.

The continuous development of sophisticated physically-based flow routing schemes coupled with land surface models allows us to easily obtain gridded water discharge time series at the global scale with reasonable accuracy. However, these modeling systems are frequently constrained by

quality or time length of global datasets, preventing one of obtaining accurate simulations of physical processes on a near real-time basis at poorly-gauged or ungauged locations. The combination of the present methodology with future altimetric and topographic missions will considerably improve the understanding of hydrological processes and streamflow estimates in unequipped basins. Ultimately, altimetry-based discharges can be used in a flow routing scheme framework to evaluate the feedback effects between the land surface and atmosphere and the vertical water and energy balances computed by LSMs.

Acknowledgements. The first author is funded by the NASA Postdoctoral Program (NPP) managed by Oak Ridge Associated Universities (ORAU). The study benefited from data made available by Agência Nacional de Águas (ANA) and by Laboratoire d'Etudes en Géophysique et Océanographie Spatiales (LEGOS). Grateful acknowledgments are due to G. Cochonneau (IRD) and M. C. Gennero (IRD) for their help in data acquisition and processing, B. Decharme (Météo-France) and R. Alkama (Météo-France) for providing ISBA outputs, and G. Schumann (JPL/NASA) and two anonymous reviewers for their valuable comments.

Edited by: W. Buytaert

References

- Alsdorf, D. E., Rodríguez, E., and Lettenmaier, D. P.: Measuring water from space, *Rev. Geophys.*, 45, RG2002, doi:10.1029/2006RG000197, 2007.
- Andreadis, K. M., Clark, E. A., Lettenmaier, D. P., and Alsdorf, D. E.: Prospects for river discharge and depth estimation through assimilation of swath-altimetry into a raster-based hydrodynamics model, *Geophys. Res. Lett.*, 34, L10403, doi:10.1029/2007GL029721, 2007.
- Bamber, J. L.: Ice sheet altimeter processing scheme, *Int. J. Remote Sens.*, 15, 925–938, 1994.
- Biancamaria, S., Hossain, F., and Lettenmaier, D. P.: Forecasting transboundary river water elevations from space, *Geophys. Res. Lett.*, 38, L11401, doi:10.1029/2011GL047290, 2011.
- Birkinshaw, S. J., O'Donnell, G. M., Moore, P., Kilsby, C. G., Fowler, H. J., and Berry, P. A. M.: Using satellite altimetry data to augment flow estimation techniques on the Mekong River, *Hydro. Process.*, 24, 3811–3825, doi:10.1002/hyp.7811, 2010.
- Chow, V. T.: *Open-Channel Hydraulics*, McGraw-Hill, 680 pp., 1959.
- Coe, M. T. and Birkett, C. M.: Calculation of river discharge and prediction of lake height from satellite radar altimetry: example for the Lake Chad basin, *Water Resour. Res.*, 40, W10205, doi:10.1029/2003WR002543, 2004.
- Crétaux, J. F., Jelinski, W., Calmant, S., Kouraev, A., Vuglinski, V., Bergé-Nguyen, M., Gennero, M.-C., Nino, F., Abarca Del Rio, R., Cazenave, A., and Maisongrande, P.: SOLS: A lake database to monitor in the Near Real Time water level and storage variations from remote sensing data, *Adv. Space Res.*, 47, 1497–1507, 2011.

- Decharme, B., Alkama, R., Douville, H., Becker, M., and Cazenave, A.: Global Evaluation of the ISBA-TRIP Continental Hydrological System, Part II: Uncertainties in River Routing Simulation Related to Flow Velocity and Groundwater Storage, *J. Hydrometeorol.*, 11, 601–617, doi:10.1175/2010JHM1212.1, 2010.
- Decharme, B., Alkama, R., Papa, F., Faroux, S., Douville, H., and Prigent, C.: Global off-line evaluation of the ISBA-TRIP flood model, *Clim. Dynam.*, 38, 1389–1412, doi:10.1007/s00382-011-1054-9, 2012.
- Di Baldassarre, G. and Montanari, A.: Uncertainty in river discharge observations: a quantitative analysis, *Hydrol. Earth Syst. Sci.*, 13, 913–921, doi:10.5194/hess-13-913-2009, 2009.
- Doll, P., Kaspar, F., and Lehner, B.: A global hydrological model for deriving water availability indicators: model tuning and validation, *J. Hydrol.*, 270, 105–134, doi:10.1016/S0022-1694(02)00283-4, 2003.
- Dottori, F., Martina, M. L. V., and Todini, E.: A dynamic rating curve approach to indirect discharge measurement, *Hydrol. Earth Syst. Sci.*, 13, 847–863, doi:10.5194/hess-13-847-2009, 2009.
- Durand, M., Andreadis, K. M., Alsdorf, D. E., Lettenmaier, D. P., Moller, D., and Wilson, M.: Estimation of bathymetric depth and slope from data assimilation of swath altimetry into a hydrodynamic model, *Geophys. Res. Lett.*, 35, L20401, doi:10.1029/2008GL034150, 2008.
- Fenton, J. D.: Rating Curves: Part 1 – Correction for Surface Slope. The Institution of Engineers, Australia, Conference on Hydraulics in Civil Engineering, 28–30 November 2001, Hobart, 309–317, 2001.
- Getirana, A. C. V.: A new automatic calibration approach based on rating curves: first results with ENVISAT altimetric data, GRACE, Remote Sensing and Ground-based Methods in Multi-Scale Hydrology, Proceedings of Symposium J-H01 held during IUGG2011 in Melbourne, Australia, July 2011, IAHS Publ., 343, 181–186, 2011.
- Getirana, A. C. V., Bonnet M. P., Roux, E., Calmant, S., Rotunno Filho, O. C., and Mansur, W. J.: Hydrological monitoring of large poorly gauged basins: a new approach based on spatial altimetry and distributed rainfall-runoff model, *J. Hydrol.*, 379, 205–219, doi:10.1016/j.jhydrol.2009.09.049, 2009.
- Getirana, A. C. V., Boone, A., Yamazaki, D., Decharme, B., Papa, F., and Mognard, N.: The Hydrological Modeling and Analysis Platform (HyMAP): evaluation in the Amazon basin, *J. Hydrometeorol.*, 13, 1641–1665, doi:10.1175/JHM-D-12-021.1, 2012.
- Jaccon, G. and Cudo, K. J.: Curva-chave: análise e tratado, DNAEE, Brasilia, Brazil, p. 273, 1989.
- Kosuth, P., Blitzkow, D., and Cochonneau, G.: Establishment of an altimetric reference network over the Amazon Basin using satellite radar altimetry (Topex Poseidon), Proceedings of 15 Years of Progress in Radar Altimetry Symposium, ESA, Venice, Italy, 2006.
- Kouraev, A. V., Zakharova, E. A., Samain, O., Mognard, N. M., and Cazenave, A.: Ob river discharge from TOPEX/Poseidon satellite altimetry (1992–2002), *Remote Sens. Environ.*, 93, 238–245, 2004.
- Kumar, S. V., Peters-Lidard, C. D., Tian, Y., Houser, P. R., Geiger, J., Olden, S., Lighty, L., Eastman, J. L., Doty, B., Dirmeyer, P., Adams, J., Mitchell, K., Wood, E. F., and Sheffield, J.: Land information system: An interoperable framework for high resolution land surface modeling, *Environ. Model. Softw.*, 21, 1402–1415, doi:10.1016/j.envsoft.2005.07.004, 2006.
- León, J. G., Calmant, S., Seyler, F., Bonnet, M. P., Cauhope, M., Frappart, F., and Fillizola, N.: Rating curves and estimation of average depth at the upper Negro river based on satellite altimeter data and modelled discharges, *J. Hydrol.*, 328, 481–496, 2006.
- Michailovsky, C. I., McEnnis, S., Berry, P. A. M., Smith, R., and Bauer-Gottwein, P.: River monitoring from satellite radar altimetry in the Zambezi River basin, *Hydrol. Earth Syst. Sci.*, 16, 2181–2192, doi:10.5194/hess-16-2181-2012, 2012.
- Noilhan, J. and Mahfouf, J. F.: The ISBA land surface parameterisation scheme, *Global Planet. Change*, 13, 145–159, doi:10.1016/0921-8181(95)00043-7, 1996.
- Rantz, S. E. et al.: Measurement and computation of streamflow, Measurement of Stage and Discharge, US Geological Survey Water Supply Paper, Washington, USA, vol. 1, p. 284, 1982.
- Silva, J. S., Calmant, S., Seyler, F., Rotunno Filho, O. C., Cochonneau, G., and Mansur, W. J.: Water levels in the Amazon basin derived from the ERS 2 and ENVISAT radar altimetry missions, *Remote Sens. Environ.*, 114, 2160–2181, 2011.
- Tapley, B. D., Bettadpur, S., Watkins, M., and Reigber, C.: The gravity recovery and climate experiment: mission overview and early results, *Geophys. Res. Lett.*, 31, L09607, doi:10.1029/2004GL019920, 2004.
- Trigg, M. A., Wilson, M. D., Bates, P. D., Horritt, M. S., Alsdorf, D. E., Forsberg, B. R., and Vega, M. C.: Amazon flood wave hydraulics, *J. Hydrol.*, 374, 92–105, doi:10.1016/j.jhydrol.2009.06.004, 2009.
- Yamazaki, D., Kanae, S., Hyungjun, K., and Oki, T.: A physically-based description of floodplain inundation dynamics in a 1 global river routing model, *Water Resour. Res.*, 47, W04501, doi:10.1029/2010WR009726, 2011.
- Zakharova, E., Kouraev, A., and Cazenave, A.: Amazon river discharge estimated from the Topex/Poseidon altimetry, *C. R. Geosci.*, 338, 188–196, 2006.